Proc. Natl. Conf. Theor. Phys. **36** (2011), pp. 239-247

STRUCTURES OF ADSORBED HALIDE ANIONS ON A COPPER ELECTRODE STUDIED BY IN SITU SCANNING TUNNELING MICROSCOPY

PHAN THANH HAI
Institute of Physical and Theoretical Chemistry, University of Bonn, Wegelerstr.12, 53115 Bonn, Germany
Department of Physics, Quynhon University, 170 An Duong Vuong, Quynhon, Vietnam
DOAN MINH THUY
Department of Physics, Quynhon University, 170 An Duong Vuong, Quynhon, Vietnam
WANDELT KLAUS
Institute of Physical and Theoretical Chemistry, University of Bonn, Wegelerstr.12, 53115 Bonn, Germany

Abstract. *The structures of adsorbed halide monolayers, e.g. chloride, iodide, on a $Cu(100)$ electrode have been investigated by a combination of cyclic voltammetry (CV) and electrochemical scanning tunneling microscopy (EC-STM). The potential range of the copper electrode in electrolytes is limited by two chemical reactions, (i) the oxidative copper dissolution reaction (CDR) at the anodic limit and (ii) the reductive hydrogen evolution reaction (HER) at the cathodic limit. While a featureless CV curve is characteristic for this electrode surface in pure hydrochloric acid, drastic changes in the CV curves are observed in the iodide containing solutions, indicating the formation of a two-dimensional CuI film. While chloride anions form a simple $c(2\times2)$ structure on the $Cu(100)$ electrode, an electrocompressible $c(p\times2)$ structure of adsorbed iodide is found, which at anodic potentials at the onset of copper dissolution transforms into the two-dimensional CuI compound. Based on these informations structure models are proposed for the various adsorbate layers which could serve as input in theoretical simulations.*

I. INTRODUCTION

In recent decades copper has attracted great attention because of its importance as a connecting material for integrated circuits in the silicon chip technology replacing the traditional vacuum deposited aluminum based interconnects [1, 2]. It is well known that the damascene copper electroplating process invented in the early 1990s at IBM [1] has changed significantly the state-of-the-art chip fabrication. A detailed understanding of the relevant interfacial properties of those devices at the nanometer-scale is still required since the control of the copper-electrolyte interfaces with or without external potential is still a particular challenge. Accordingly, a detailed comprehension from the theoretical and experimental points of view on an atomic scale of the role of additives on copper plating [3, 4, 5, 6], copper corrosion, corrosion inhibition by organic molecules [7, 8], oxidation, anodic dissolution [9, 10], and passive film formation [11, 12, 13, 14, 15] is, hence, of fundamental interest.

Experimentally, scanning tunneling microscopy (STM) invented in the early 1980s by Binnig and Rohrer [16, 17, 18] is a powerful tool for the investigation of atomic scale surface structures formed in UHV environments. Shortly after, for the first time by Sonnenfeld and Hansma in 1986 [19], the in situ visualization of surface dynamics and thermodynamical processes, e.g. corrosion, electrodeposition, adsorption, as well as surface modification and passivation, via STM measurements in electrochemical media has resulted in a radical change in surface electrochemistry. Later a few other research groups have come up with further developments of electrochemical STMs (EC-STM) in order to gain better research results. Exemplarily, a home-built EC-STM system introduced by Wilms et al. in 1999 [20] has been applied since then by the Wandelt group, University of Bonn, very successfully. At presence, several other research groups worldwide are using this equipment from Bonn for their studies, such as the groups of Broekmann (Uni. Bern) [21], De Feyter (Uni. Leuven) [22], Krupsky (Uni. Wroclaw), Nowakowski (Pol. Academy of Sciences, Warsaw), Tsay (University of Technology, Taipei), etc.,..

In the present contribution, the interaction of chloride and iodide anions with the surface of a $Cu(100)$ electrode is studied with this EC-STM. The high resolution data are presented here and discussed in detail. While chloride forms a highly ordered $c(2 \times 2)$ structure within the double layer regime of the copper potential window, iodide adsorption leads to a variety of incommensurate adlayers as well as the formation of a two dimensional copper iodide compound film.

II. EXPERIMENTAL SETUP

For all solutions, high purity water (Milli-Q purification system, conductivity $>$ 18 $M\Omega.cm$, TOC $<$ 4 ppb), halides purchased from Aldrich-Sigma (Germany) and other reagent grade chemicals were used. All electrolyte solutions were purged with oxygen free argon gas for several hours before use. The potential of the copper electrode is referenced to a reversible hydrogen electrode (RHE) while a Pt wire is employed as counter-electrode.

In order to guarantee a reproducibly smooth surface even after several electropolishing cycles, a surface orientation of less than 0.5^o off the $Cu(100)$ plane was required (MaTechCompany, Juelich, Germany). The $Cu(100)$ sample was electropolished before each STM experiment in order to remove the native oxide film formed in air and contaminations on the surface by immersing the electrode surface into 50% orthophosphoric acid. Subsequently, an anodic potential of $2V$ was applied between the copper electrode and a platinum foil for about 20 to 40s. After this etching procedure the copper surface was rinsed with degassed 10 mM hydrochloric acid solution and mounted into the electrochemical cell of the home-built electrochemical scanning tunneling microscopy (EC-STM) described in detail by Wilms et al. [20]

In order to eliminate the influence of oxygen as well as acoustic and electromagnetic interferences from all cyclic voltammogram (CV) and EC-STM measurements, the whole EC-STM system is housed within a sealed aluminium chamber with electrical and liquid feed-throughs and filled with suprapure argon gas. Initial CV and STM measurements were performed in HCl electrolyte in order to investigate the electrochemistry and adsorbate structure of chloride anions on the $Cu(100)$ electrode. For the adsorption of iodide anions on the same substrate surface the supporting electrolyte (10 mM HCl) was replaced by

a solution containing iodide ($10\ mM\ HCl + 1\ mM\ KI$) at a potential of $-100\ mV$ vs RHE to avoid $3D\ CuI$ formation from solution (see below).

The tunneling tips used in our experiments were electrochemically etched from a $0.25\ mm$ tungsten wire in $2M\ KOH$ solution and subsequently coated by passing the tip through a hot-melt glue film.

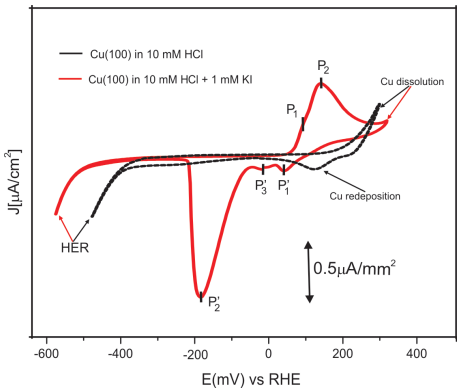

Fig. 1. Cyclic voltammograms of a $Cu(100)$ electrode in pure hydrochloric acid (dash back curve) and in iodide containing HCl electrolyte (red curve).

III. RESULTS AND DISCUSSION

III.1. Electrochemistry

The electrochemistry of the $Cu(100)$ electrode in the electrolytes containing chloride and iodide anions, firstly, has been investigated by mean of cyclic voltametry (CV) as shown in Fig. 1. The potential range of the copper electrode in electrolytes is limited by two chemical reactions, (i) the oxidative copper dissolution reaction (CDR) at the anodic limit and (ii) the reductive hydrogen evolution reaction (HER) at the cathodic limit. A featureless CV curve (dash-black curve) is characteristic for $Cu(100)$ in pure hydrochloric acid showing a cathodic peak (actually an unresolved double-peak) at $+130\ mV$ assigned to the redeposition of dissolved copper cations from solution following the sequence: $Cu^{2+} \rightarrow Cu^{+} \rightarrow Cu^{o}$ [23-24]. In comparison with this CV, a drastic change in the CV curve is observed once the $Cu(100)$ is brought into contact with the iodide anions containing solution (red curve). The most striking deviation from the pure supporting electrolyte CV, in fact, is seen in the anodic potential regime. As a consequence, some characteristic features are visible in the anodic scan direction labeled $P_1 = +90\ mV$ and $P_2 = +141\ mV$, respectively. These peaks are from the electrochemical point of view assigned to the formation of new phases from iodide anions in the solution and the cuprous and/or cupric cations from the copper dissolution at positive potentials. As a result, a $2D\ CuI$ film at P_1 and $3D\ CuI$ clusters at P_2 are formed ontop of an adsorbed iodide interlayer according to the following equations [23, 24, 25]

$$Cu^{+} + I^{-} \longleftrightarrow CuI_{monomer}\ , \tag{1}$$

$$nCuI \longleftrightarrow (CuI)_n \ (film) \ . \tag{2}$$

In the reverse scan several cathodic current waves emerge relating to complicated surface processes. The two first bumps, i.e. the features labeled $P_1^{'} = +45\ mV$ and $P_3^{'} = -10\ mV$ are formed due to the dissolution of the $2D\ CuI$ film, the highly intensive peak $P_2^{'}$ at $E = -190\ mV$ arises from the reduction of the $3D\ CuI$ clusters which precipitated from the solution phase onto the copper surface following a process described by the following [23]:

$$2Cu^{2+} + 4I^{-} \longleftrightarrow 2CuI \downarrow + I_2 \downarrow \ . \tag{3}$$

The molecular iodine formed in (3), however, is not stable under the current conditions, and, therefore, should be electroreduced to iodide anions according to [24]:

$$I_2 + 2e^{-} \longrightarrow 2I^{-} \ (electroreduction) \ . \tag{4}$$

The same results and reasonable explanations have been reported by Inukai et al. [26] who observed similar CV results of $Cu(100)$ exposed to an iodide containing perchloric acid, and by Broekmann et al. [23] who used the same working electrolyte as in the present work.

III.2. Morphology and atomic structure of chloride modified $Cu(100)$ electrode

It is well known that chloride anions are adsorbing strongly on a $Cu(100)$ electrode in order to form a highly ordered $(\sqrt{2} \times \sqrt{2})R45^o$ superstructure within the whole potential range of the copper potential window that can be investigated by in situ STM measurements. Equivalently, this structure can be also described by a $c(2 \times 2)$ unit cell. Fig. 2 depicts the surface morphology of the $Cu(100)$ electrode exposed to hydrochloric acid solution at a potential of $+20\ mV$ vs HRE. The STM results show that the chloride adsorbate induces a significant change in the surface morphology of the $Cu(100)$ electrode due to a strong substrate-adsorbate interaction leading to a new topographic equilibrium of the surface stabilized by chloride anions at copper steps aligned along the [001] and [010] directions [27, 28]. In order to precisely clarify the arrangement of the chloride anions at an atomic scale high resolution STM images are shown in Fig. 3. Obviously, the chloride anions oriented parallel to the step-edges result in step edges which appear perfectly straight and atomically smooth (Fig. 2 and Fig. 3a) indicating that defects such as kink sites are drastically disfavored. The detailed surface structure of the chloride terminated $Cu(100)$ electrode on an atomic level with the typical quadratic features of the $(\sqrt{2} \times \sqrt{2})R45^o$ superstructure and a corresponding hard sphere model depicting two successive layers and the unit cell are presented in Fig. 3b and Fig. 3c. The lattice constants calculated are times longer than the nearest neighbor distance of copper atoms on the $Cu(100)$ surface, namely 3.6 ± 0.1 Å[27].

III.3. Structural characterization of iodide adlayer on the $Cu(100)$ electrode

An electrolyte replacement procedure from pure to iodide containing hydrochloric acid as mentioned in the experimental section immediately results in the formation of a new laterally ordered phase i.e. an iodide adlayer as described in Fig. 4. Unlike the $c(2\times2)-Cl$ structure, iodide anions form a distorted structure which is solely commensurate along the

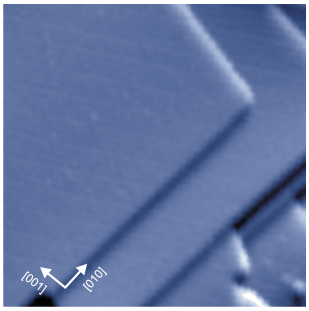

Fig. 2. Morphologic feature of a chloride adlayer on a $Cu(100)$ electrode surface, 83.23 $nm \times 83.23$ nm, $Ubias = +168$ mV, $It = 0.1$ nA, $E = +20$ mV.

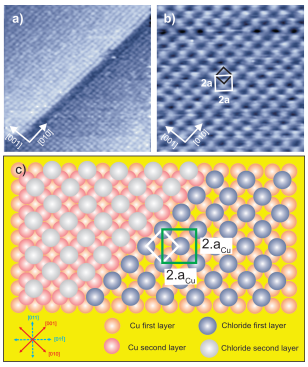

Fig. 3. High resolution STM images of chloride covered $Cu(100)$ electrode surface: a) typical copper steps preferentially aligned parallel to the close packed chloride rows, 9.92 $nm \times 9.92$ nm, $Ubias = +40$ mV, $It = 5$ nA, $E = +20$ mV; b) $c(2 \times 2) - Cl$ structure on $Cu(100)$, 4.37 $nm \times 4.37$ nm, $Ubias = +20$ mV, $It = 2.5$ nA, $E = -10$ mV; c) structural model of the $c(2 \times 2) - Cl$ adlayer.

$< 011 >$ substrate directions [29, 30, 31] leading to a one dimensional height modulation as shown in Figs. 4a-b. Obviously, this structure derives from the quadratic chloride structure on the $Cu(100)$ substrate by expanding it parallel to only one of the original unit cell vectors. As a result, the iodide unit cell is described by a $c(p \times 2) - I$ notation with the p value varying proportionally to the electrode potential in terms of a so called electro-expansion/-compression process. A possible structure model of the $c(p \times 2) - I$ lattice is presented in Fig.4c with the surface coverage being about 0.4 ML and a nearest neighbor distance (NND) of 4.1 Å at the given potential [23].

An advantage of STM measurements in electrochemical environment compared to those in UHV is the additional control of the surface processes by adjusting the electrode potential. In the present study, a series of EC-STM images has been recorded at the same surface area with a continuously positive adjustment of the electrode potential. As can be seen in Fig. 5, a local dissolution of copper material is preferentially taking place at step-edges when the electrode potential is swept from $E = +90$ mV to $E = +120$ mV vs

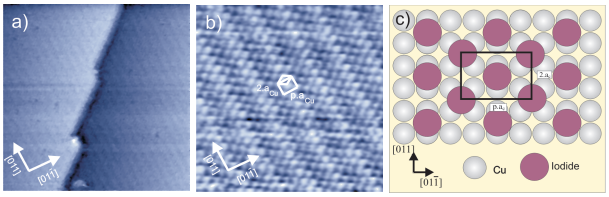

Fig. 4. Atomic structure and surface morphology of the iodide modified $Cu(100)$ electrode surface: a) height modulation of the iodide structure, 28.81 $nm \times$ 28.81 nm, $Ubias = +278\ mV$, $It = 0.15\ nA$, $E = +20\ mV$; b) atomic structure of the $c(p \times 2) - I$ layer, $Ubias = +20\ mV$, $It = 1.2\ nA$, $E = 0\ mV$, c) structure model of $c(p \times 2) - I$ adlayer, p varies with the electrode potential.

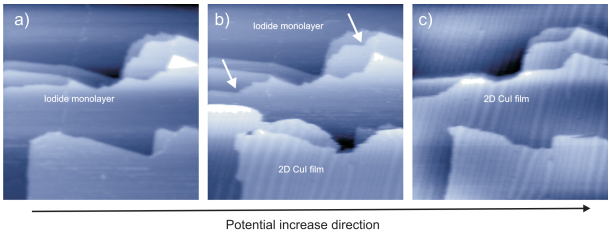

Fig. 5. Simultaneously occurring copper dissolution and $2D\ CuI$ growth on a $Cu(100)$ electrode surface, 72.02 $nm \times 72.02\ nm$; a) adsorbed iodide mono-film layer (phase I), $Ubias = 112\ mV$, $It = 0.3\ nA$, $E = +90\ mV$; b) mixed structure between iodide adlayer and CuI film phase II, $Ubias = 112\ mV$, $It = 0.3\ nA$, $E = +120\ mV$; c) fully developed CuI film on $Cu(100)$ surface, $Ubias = 112\ mV$, $It = 0.3\ nA$, $E = +135\ mV$.

RHE (Figs. 5a-b) as marked by white arrows. Astonishingly, simultaneously to the local removal of copper from the step-edges one can observe the growth of a new ordered stripe structure ontop of the $c(p \times 2) - I$ interlayer (Fig. 5b) indicating that both processes i.e. copper dissolution and stripe formation are correlated with each other. A full monolayer of the new stripe phase rapidly covers the entire electrode surface as presented in Fig. 5c. Obviously, the lateral structure of this new overlayer significantly differs from the well known $c(p \times 2) - I$ phase on the $Cu(100)$ substrate. Based on the observed consumption of copper this new phase has been assigned to a $2D$ film growing ontop of the iodide precovered $Cu(100)$ [24]. To accentuate the new structure of this film a close-up view at the atomic level is shown at the initial and final stage of the film formation in Figs. 6-8, respectively. The obtained STM results suggest that the initially formed phase is not stable at any potential and must, therefore, be considered as a metastable phase denoted by phase II (Fig. 6). Large scale and high resolution figures of this initial phase II are described in Fig. 7. The iodide anions are arranged in a stripe pattern with a height modulation and periodicity calculated to be about $0.07 \pm 0.01\ nm$ and $L = 3.75 \pm 0.1\ nm$, respectively. Nevertheless, after the formation, this metastable phase II is immediately transformed into a more permanent pattern within an actually narrow potential window between $+120\ mV$ to $+140\ mV$, namely the so-called phase III. The surface dynamics

of this phase transition is presented in Fig. 8. The new phase III shows also a stripe structure but with a significantly lower height modulation and is rotated with respect

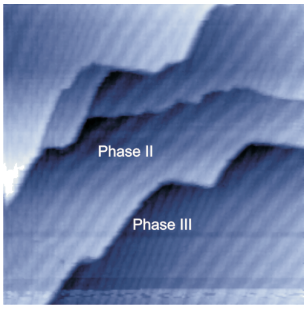

Fig. 6. Typical large scale STM image of CuI phases with different height corrugations formed on the iodide modified $Cu(100)$ electrode surface, 72.02 $nm \times$ 72.02 nm, $Ubias = 190\ mV$, $It = 0.4\ nA$, $E = +127\ mV$.

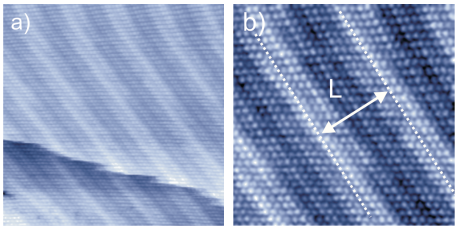

Fig. 7. Medium scale and high resolution STM images of the metastable CuI phase (phase II): a) 28.8 $nm \times 28.81\ nm$, $Ubias = 210\ mV$, $It = 0.5\ nA$, $E = +127\ mV$; b) 12.83 $nm \times 12.83\ nm$, $Ubias = 112\ mV$, $It = 0.3\ nA$, $E = +130\ mV$.

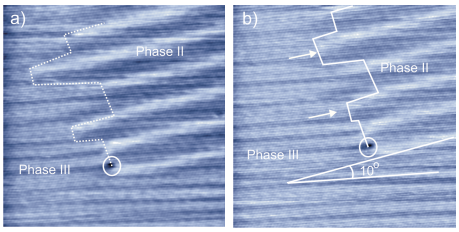

Fig. 8. Surface dynamics of the phase transition from metastable phase (phase II) to stable pattern (phase III): 28.82 $nm \times 28.81nm$, $Ubias = 200\ mV$, $It = 0.6\ nA$; a) $E = +132\ mV$; b) $E = +135\ mV$.

to phase II by an angle of 10^o (Fig. 8b). Unlike phase II two different stripe widths are formed in phase III, namely $L_1 = 1.69 \pm 0.1\ nm$ and $L_2 = 2.18 \pm 0.1\ nm$, respectively, as seen in Fig. 9a. The same ECSTM results have already been obtained by Broekmann et al. [23] and Hai et al. [32], but no definitive structure models have been presented

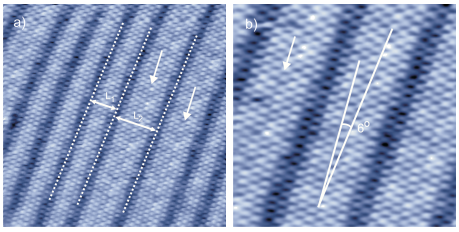

Fig. 9. Atomic structure of the stable CuI film (phase III): a) 12.76 $nm \times 12.76$ nm and b) 7.09 $nm \times 7.09$ nm, $Ubias = 140$ mV, $It = 0.3$ nA, $E = +138$ mV (note very shallow depression in the middle of the broad stripes marked by white arrows).

so far explaining the structural details and differences of both phases. In any case, the unidirectional modulation across the stripes is related to a lattice mismatch between the $2D$ CuI film and the substrate underneath.

The high resolution images of CuI phase III in Fig.9 show an almost ideal hexagonal symmetry with a NND of 0.47 ± 0.02 nm. Moreover, the stripe propagation directions are rotated by an angle of 6 ± 1^o with respect to the close-packed rows (Fig. 9b) of atoms visible within the stripes. On average the narrow stripes are four atoms wide while the broad stripes are 7 atomic rows broad. It is suggested that the broad stripe are actually two joint narrow stripes as suggested by a very shallow depression in the middle of the broad stripes (white arrows in Fig. 9a).

Sweeping the electrode potential more positively the copper dissolution is first accelerated but then drastically slowed down when the potential is over $E = +135$ mV. As a result, $3D$ CuI clusters appear on the copper surface with the result that the surface imaging becomes more and more difficult due to the low conductivity of bulky CuI cluster (STM figure not shown in this context).

IV. CONCLUSION

The electrochemical behaviors of a $Cu(100)$ electrode in pure dilute HCl and iodide containing HCl solutions was investigated by in situ STM. Halide anions adsorb with typical structures on the $Cu(100)$ electrode surface. While a $c(2 \times 2)$ structure is found for the chloride adlayer, variable potential dependent structures are observed in the iodide adsorption case. A distorted $c(2 \times 2)$ structure or a so-called $c(p \times 2) - I$, with p varying proportionally with the electrode potential, was found at potentials less than $E = +90$ mV vs RHE. In contrast, new phases were indentified in the potential range from $+120$ mV to $+140$ mV where copper dissolution taken place and a CuI film compound is formed. Ultimately, an ideal hexagonal $2D$ CuI structure (phase III) is stably formed after overcoming a pseudo hexagonal pattern (phase II) at the initial stage of the new phase formation.

ACKNOWLEDGMENT

The financial support by the Deutsche Forschungsgemeinschaft (DFG) through the SFB 624 project is gratefully acknowledged.

REFERENCES

[1] P. C. Andriacos, C. Uzoh, J. O. Ducovic, J. Horcans, H. Deligianni, *IBM J. Res. Dev.* **42** (1998) 567.
[2] L. Arnaud, G. Tartavel, T. Berger, D. Mariolle, Y. Gobil, I. Touet, *Microelectron. Reliab.* **40** (2000) 1295.
[3] K. Kondo, N. Yamakawa, Z. Tanaka, K. Hayashi, *J. Electroanal. Chem.* **559** (2003) 137.
[4] J. J. Kelly, A. C. West, *J. Electrochem. Soc.* **145** (1998) 3472.
[5] J. J. Kelly, A. C. West, *J. Electrochem. Soc.* **145** (1998) 3477.
[6] J. J. Kelly, C. Tian, A. C. West, *J. Electrochem. Soc.* **146** (1999) 2540.
[7] M. R. Vogt, R. J. Nichols, O. M. Magnussen, R. J. Behm, *J. Phys. Chem. B* **102** (1998) 5859.
[8] O. M. Magnussen, M. R. Vogt, J. Scherer, A. Lachenwitzer, R. Behm, *J. Mater Corros.* **49** (1998) 169.
[9] D. W. Suggs, A. J Bard, *J. Phys. Chem.* **99** (1995) 8349.
[10] M. R. Vogt, A. Lachenwitzer, O. M. Magnussen, R. Behm, *J. Surf. Sci.* **399** (1998) 49.
[11] V. Maurice, H. H. Strehblow, P. Marcus, *J. Electrochem. Soc.* **146** (1999) 524.
[12] V. Maurice, H. H. Strehblow, P. Marcus, *J. Surf. Sci.* **458** (2000) 185.
[13] H. H. Strehblow, V. Maurice, P. Marcus, *Electrochim. Acta* **46** (2001) 3755.
[14] J. Kunze, V. Maurice, L. H. Klein, H. H. Strehblow, P. Marcus, *J. Electroanal. Chem.* **113** (2003) 554.
[15] J. Kunze, V. Maurice, L. H. Klein, H. H. Strehblow, P. Marcus, *Corros. Sci.* **46** (2004) 245.
[16] G. Binnig, H. Rohrer, *Surf. Sci.* **126** (1983) 236.
[17] G. Binnig, H. Rohrer, C. Gerber, E. Weibel, *Appl. Phys. Lett.* **40** (1982) 178.
[18] G. Binnig, H. Rohrer, *Scientific American* **253** (1985) 50.
[19] R. Sonnenfeld, P. K. Hansma, *Science* **232** (1986) 211.
[20] M. Wilms, M. Kruft, G. Bermes, K. Wandelt, *Rev. Sci. 1999. Instr.* **70** (1999) 3641.
[21] P. Broekmann, A. Fluegel, C. Emnet, M. Arnold, C. Roeger-Goepfert, A. Wagner, N.T.M. Hai, D. Mayer, *Electrochim. Acta* **56** (2011) 4724.
[22] N. T. M. Hai, S. Furukawa, T. Vosch, S. De Feyter, P. Broekmann, K. Wandelt, *Phys. Chem. Chem. Phys.* **11** (2009) 5422.
[23] P. Broekmann, N.T.M. Hai, and K. Wandelt, *J. Appl. Elect. Chem.*, **36** (2006) 1241.
[24] N. T. M. Hai, S. Huemann, R. Hunger, W. Jaegermann, K. Wandelt, P. Broekmann, *J. Phys. Chem. C* **111** (2007) 14768.
[25] P. Broekmann, N. T. M. Hai, K. Wandelt, *Surf. Sci.* **600** (2006) 3971.
[26] J. Inukai, Y. Osawa, K. Itaya, *J. Phys. Chem. B* **102** (1998) 10034.
[27] S. Huemann, N. T. M. Hai, P. Broekmann, K. Wandelt, *J. Phys. Chem. B 110* (2006) 24955.
[28] T. H. Phan, K. Wandelt, unpublished
[29] P. Broekmann, A. Spaenig, A. Hommes, K. Wandelt, *Surf. Sci.* **517** (2002) 123.
[30] A. Hommes, A. Spaenig, P. Broekmann, K. Wandelt, *Surf. Sci.* **547** (2003) 239.
[31] T. H. Phan, K. Wandelt, unpublished
[32] N. T. M. Hai, PhD dissertation (2007), Born.

Received 30-09-2011.